

1 **Identification of nitrogen-dependent QTL and underlying genes**
2 **for root system architecture in hexaploid wheat**

3 Marcus Griffiths^{1,2}, Jonathan A. Atkinson¹, Laura-Jayne Gardiner³, Ranjan Swarup¹, Michael
4 P. Pound⁴, Michael H. Wilson¹, Malcolm J. Bennett¹ & Darren M. Wells^{1*}.

5 ¹School of Biosciences, University of Nottingham, Loughborough, LE12 5RD, UK.

6 ²Noble Research Institute, Ardmore, Oklahoma, 73401, US.

7 ³IBM Research, Warrington, WA4 4AD, UK.

8 ⁴School of Computer Science, University of Nottingham, Nottingham, NG8 1BB, UK.

9

10 *Correspondence to DMW.

11 e-mail: darren.wells@nottingham.ac.uk

12

13 Date of submission – 27 March 2019

14 No. words in abstract – 157

15 No. words in main text – 3370

16 No. tables – 4

17 No. figures – 3

18 Supplementary Data – 2 tables, 2 figures

19

20 M. Griffiths: mdgriffiths@noble.org ORCID iD: 0000-0003-2349-8967

21 J. A. Atkinson: jonathan.atkinson@nottingham.ac.uk ORCID iD: 0000-0003-2815-0812

22 L. J. Gardiner: laura-jayne.gardiner@ibm.com ORCID iD: 0000-0002-9177-4452

23 R. Swarup: ranjan.swarup@nottingham.ac.uk ORCID iD: 0000-0002-6438-9188

24 M. P. Pound: michael.pound@nottingham.ac.uk ORCID iD: 0000-0002-5016-1078

25 M. H. Wilson: michael.wilson@nottingham.ac.uk ORCID iD: 0000-0002-6323-6059

26 M. J. Bennett: malcolm.bennett@nottingham.ac.uk ORCID iD: 0000-0003-0475-390X

27 D. M. Wells: darren.wells@nottingham.ac.uk Tel. +44 115 951 6373 ORCID iD: 0000-0002-
28 4246-4909

29

30 Running title – Nitrogen-dependent wheat root QTLs and underlying genes.

31 **Highlight**

32 Using a hydroponic pouch phenotyping system, nitrogen-dependent root QTLs were
33 identified in wheat. For a candidate N-dependent root angle QTL an upregulated NPF family
34 gene was identified likely transporting nitrate or ABA as part of a N-dependent response
35 affecting root angle.

36 **Abstract**

37 The root system architecture (RSA) of a crop has a profound effect on the uptake of nutrients
38 and consequently the potential yield. However, little is known about the genetic basis of RSA
39 and resource dependent response in wheat (*Triticum aestivum* L.). Here, a high-throughput
40 hydroponic root phenotyping system was used to identify N-dependent root traits in a wheat
41 mapping population. Using quantitative trait locus (QTL) analysis, a total of 55 QTLs were
42 discovered for seedling root traits across two N treatments, 25 of which were N-dependent.
43 Transcriptomic analyses were used on a N-dependent root angle QTL on chromosome 2D
44 and 17 candidate genes were identified. Of these N-dependent genes a nitrate transporter
45 1/peptide transporter (NPF) family gene was upregulated making it an interesting candidate
46 for N signalling and response processes for root angle change. The RNA-seq results provide
47 valuable genetic insight for root angle control, N-dependent responses and candidate genes
48 for improvement of N capture in wheat.

49 **Key Words**

50 RNA-seq, Root angle, Root system architecture, Savannah Rialto doubled-haploid
51 population, QTL, Nitrate, Nitrogen, NPF, wheat.

52 **Abbreviations**

53 ABA, Abscisic acid; BLUEs, best linear unbiased estimates; BLUPS, best linear unbiased
54 predictions; DAG, days after germination; DH, doubled haploid; LOD, logarithm of odds;
55 nabim, National Association of British & Irish Millers; NPF, peptide transporter family;
56 NRT, nitrate transporter; NUE; nitrogen use efficiency; PTR, proton-dependent oligopeptide
57 transporter; QTL, quantitative trait locus; RNA-seq, RNA sequencing technology; RSA, root
58 system architecture; RSML, Root System Markup Language.

59 **Introduction**

60 Nitrogen (N) is an essential macronutrient for plant growth and development with agriculture
61 greatly dependent on synthetic N fertilisers for enhancing productivity. Global demand for
62 fertilisers is projected to rise by 1.5% each year reaching 201.7 million tonnes in 2020, over
63 half of which is for nitrate fertilizers (118.8 million tonnes) (FAO, 2017). However, there are
64 compelling economic and environmental reasons to reduce N fertiliser use in agriculture,
65 particularly as the N fixing process is reliant on unsustainable fossil fuels (Dawson *et al.*,
66 2008).

67

68 The availability of nutrients is spatially and temporally heterogeneous in the soil. Roots
69 therefore need to forage for such resources. The spatial arrangement of the root system, called
70 the root system architecture (RSA) (Hodge *et al.*, 2009), has a profound effect on the uptake
71 of nutrients and consequently the potential yield. Optimisation of the RSA could significantly
72 improve the efficiency of resource acquisition and in turn increase the yield potential of the
73 crop. An improvement in N use efficiency (NUE) by just 1% could reduce fertiliser losses
74 and save ~\$1.1 billion annually (Delogu *et al.*, 1998; Kant *et al.*, 2010).

75 Understanding the contribution of root traits to root system architecture and function is of
76 importance for crop improvement. Artificial growth systems are widely used in plant
77 phenotyping as they are generally high throughput, allow precise control of environmental
78 parameters and are easy to replicate. Using these systems quantitative trait loci (QTL) have
79 been identified in major crops for root system architectural traits (Ren *et al.*, 2012; Clark *et al.*,
80 2013; Atkinson *et al.*, 2015; Zurek *et al.*, 2015). Understanding the genetic basis of RSA
81 in cereals is very complex and therefore identifying QTL is useful for precisely linking
82 phenotypes to regions of a chromosome. With the development of high-throughput RNA
83 sequencing technology (RNA-seq), identified QTL can now be further dissected to the gene
84 level. Using RNA-seq, a substantial number of genes and novel transcripts have been
85 identified in cereal crops including rice, sorghum, maize and wheat (Oono *et al.*, 2013; Gelli
86 *et al.*, 2014; Akpinar *et al.*, 2015; Yu *et al.*, 2015). To our knowledge, there are no other
87 studies that have identified genes related to nitrate response or root angle change in wheat.

88

89 The aim of this study was to identify root traits and genes that relate to N uptake and
90 plasticity. To achieve this a germination paper-based system was used to phenotype a wheat

91 doubled haploid (DH) mapping population under two N regimes. Here were present genomic
92 regions and underlying genes that we propose may control a N-dependent root angle response
93 in wheat.

94 **Materials and methods**

95 *Plant materials*

96 A winter wheat doubled haploid mapping population comprised of 94 lines was used for root
97 phenotyping. The population was derived from a cross between cultivars Savannah and
98 Rialto F1 plants (Limagrain UK Ltd, Rothwell, UK). Both parents are UK winter wheat
99 cultivars that were on the AHDB recommended list. Savannah is a National Association of
100 British & Irish Millers (nabim) Group 4 feed cultivar first released in 1998. Rialto is nabim
101 Group 2 bread-making cultivar first released in 1995.

102 *Seedling phenotyping*

103 Wheat seedlings were grown hydroponically using the system described in Atkinson *et al.*
104 (2015) (Fig. S1). Seeds from the Savannah × Rialto doubled haploid (S×R DH) mapping
105 population were sieved to a seed size range of 2.8–3.35 mm based on mean parental seed
106 size. Seeds were surface sterilised in 5% (v/v) sodium hypochlorite for 12 minutes before
107 three washes in dH₂O. Sterilised seeds were laid on wet germination paper (Anchor Paper
108 Company, St Paul, MN, USA) and stratified at 4°C in a dark controlled environment room
109 for 5 days. After stratification seeds were transferred to a controlled environment room at
110 20/15°C, 12 hour photoperiod, 400 $\mu\text{mol m}^{-2} \text{s}^{-1}$ PAR and kept in a light-tight container.
111 After 48 hours uniformly germinated seedlings with ~5 mm radicle length were transferred to
112 vertically orientated seedling pouches.

113

114 Seeds for 94 lines from the S×R DH mapping population were grown hydroponically either
115 in high N (3.13 mM NO₃⁻) or low N (0.23 mM NO₃⁻) modified Hoagland's solution (Table
116 S1). The experimental design was a randomised block comprised of 94 genotypes split over
117 11 experimental runs with a target of 20 replications per genotype ($n = 8 - 36$). Roots and
118 shoots of each seedling were individually imaged 10 days after germination (DAG) resulting
119 in 6924 images. The root system architecture of each seedling was extracted from the images
120 and stored in Root System Markup Language (RSML, Lobet *et al.*, 2015) using the root
121 tracing software RootNav (Pound *et al.*, 2013). Root traits were quantified using RootNav
122 standard functions and additional measurements as described in Atkinson *et al.* (2015). The
123 shoot length and area were extracted from the shoot images using the colour threshold tool in
124 FIJI software package (Schindelin *et al.*, 2012).

125 *Quantitative trait locus mapping*

126 Detection of QTL was conducted using the R Statistics package “R/qrtl” (Broman *et al.*,
127 2003). The map used was a high-density Savannah × Rialto iSelect map obtained from Wang
128 *et al.* (2013) with redundant and closer than 0.5 cM markers stripped out. Before data
129 processing, the best linear unbiased estimates (BLUEs) or best linear unbiased predictions
130 (BLUPs) were calculated for the traits if necessary. QTL were identified based on the
131 extended Haley-Knott algorithm (Haley & Knott, 1992). The threshold logarithm of the odds
132 (LOD) scores were calculated by 1000 × permutation test at $p < 0.05$ level (Churchill &
133 Doerge, 1994). The threshold for declaring presence of a QTL was a LOD score of 2.0. The
134 annotated linkage map was generated using R Statistics package “LinkageMapView”
135 (Ouellette *et al.*, 2018).

136 *RNA-sequencing of candidate QTL*

137 RNA-seq was used to identify underlying genes for a candidate QTL with expression levels
138 changed by N treatment. For the candidate QTL two pooled root samples were immediately
139 frozen after collection using liquid nitrogen and stored at -80°C. Each pool was made up
140 from four individual lines (3 plants per line), one pool was comprised of lines that had the
141 candidate QTL (Group A) and the second pool did not have the QTL (Group B). The lines
142 were selected based on largest phenotypic differences for trait associated with candidate
143 QTL. 500–1000 mg of frozen root tissue was homogenised using a pestle and mortar with
144 liquid nitrogen. The homogenised tissue powder was then transferred to a 2 mL
145 microcentrifuge tube and 1 mL of TRIzol© reagent added. The sample was homogenised and
146 incubated at room temperature for 5 minutes to permit complete dissociation of the
147 nucleoprotein complex. 200 µL of chloroform was added and the tube shaken vigorously for
148 15 seconds for phase separation. The tube was then incubated for 2–3 minutes at room
149 temperature before centrifuged at 13000 × g at 4°C for 5 minutes. After centrifugation, 500
150 µL of the aqueous phase was transferred to an RNase-free tube with 250 µL 70% ethanol and
151 vortexed. Once settled the pellet was removed and resuspended in 1000 µL of RNase-free
152 water. To analyse RNA quality and purity 1 µL of nucleic acid sample was quantified using a
153 NanoDrop™ 2000c with values above 500 ng µL⁻¹ or higher accepted. The samples were
154 then stored at -80°C for RNA-seq. Illumina Paired-End Multiplexed RNA sequencing was
155 performed by Source Bioscience (Nottingham, UK).

156

157 Differential gene expression analysis was conducted using the IWGSC RefSeq v1.1 assembly
158 (International Wheat Genome Sequencing Consortium, 2018)
159 (http://plants.ensembl.org/Triticum_aestivum/) and the TGAC v1 Chinese Spring reference
160 sequence (Clavijo *et al.*, 2017). Raw sequencing reads were trimmed for adapter sequence
161 and for regions where the average quality per base dropped below 15 (Trimmomatic version
162 0.32) (Bolger *et al.*, 2014). After trimming, reads below 40 bp were eliminated from the
163 dataset. Trimmed reads were aligned to the reference sequences assembly using splice-aware
164 aligner HISAT2 (Pertea *et al.*, 2016). Uniquely mapped reads were selected, and duplicate
165 reads filtered out. Unmapped reads across all samples were assembled into transcripts using
166 MaSuRCA software and sequences 250 bp or larger taken forward (Zimin *et al.*, 2013).
167 Unmapped reads were re-aligned to these assembled transcripts individually and added to
168 their sample specific reads while the assembled transcripts were combined with the reference
169 sequence and GTF annotation for downstream investigations. StringTie software was used to
170 calculate gene and transcript abundances for each sample across the analysis specific
171 annotated genes (Pertea *et al.*, 2016). Finally, DEseq was used to visualise results and
172 identify differential expression between samples (Anders & Huber, 2010). Differentially
173 expressed genes were compared between the IWGSC RefSeq v1.1 and TGAC v1 reference
174 assemblies to identify overlap using BLAST (BLASTN, e-value 1e-05, identity 95%,
175 minimum length 40bp) (Altschul *et al.*, 1990). The top matches for each gene between the
176 reference sequences were used to allow an integrative and comprehensive annotation of
177 genes.

178 *Phylogenetic analysis*

179 A phylogenetic analysis of protein families was conducted to compare the protein sequences
180 of *A. thaliana*, *O. sativa* L. and *T. aestivum* L. proton-dependent oligopeptide transporter
181 (NPF) families (also known as the NRT1/PTR family). *A. thaliana* sequences were obtained
182 from (Léran *et al.*, 2014). Using the latest genome for *T. aestivum* L. (IWGSC RefSeq v1.1
183 assembly) and *O. sativa* L. (MSU Release 7.0, Kawahara *et al.*, 2013,
184 <https://phytozome.jgi.doe.gov/>) a HMM profile search was conducted (Krogh *et al.*, 2001).
185 The resulting list of proteins were scanned using Pfam (El-Gebali *et al.*, 2019). Only single
186 gene models of candidate genes with PTR2 domains were retained. The protein sequences
187 were used to generate a maximum-likelihood tree using the software RAXML (Stamatakis,
188 2014). The exported tree file (.NWK) was then visualised using the R package “ggtree” (Yu

189 *et al.*, 2017) and used for phylogenetic tree construction. The exported tree file (.NWK) was
190 visualised using the R package “ggtree” (Yu *et al.*, 2017).

191 **Results**

192 *Root phenotypic variation in a wheat double haploid population*

193 The phenotypic trait values for the parental lines, Savannah and Rialto, under two N regimes
194 are summarised in Table 2. Significant differences between the parents were observed in root
195 traits only with no significant shoot length or shoot area differences ($p = ns$). For the root
196 traits measured, differential responses to N treatment were also observed (Fig. 1 a-c). For all
197 root length and size traits (except for lateral root length under low N) Savannah was
198 significantly larger ($p < 0.05$) than Rialto under both high and low N treatments. There was
199 no significant effect of N supply on root traits in Rialto except for a reduction in seminal root
200 count. Savannah, however, showed significant reduction in lateral root length, convex hull
201 area and maximum root depth under low N. There were no significant root angle differences
202 between the parents or N treatments. Lines within the Savannah \times Rialto (S \times R) DH
203 population showed transgressive segregation with trait values more extreme than the parents
204 (Fig. 1 a-c).

205 *Root QTL detection in the S \times R DH population*

206 A total of 55 QTLs were discovered for seedling root traits across both N treatments (Fig. 2,
207 Table 3), of which 36 came from Savannah, and 19 from Rialto. QTLs were found on
208 chromosomes 1A, 1B, 2D, 3B, 4D, 6D, 7A and 7D, with 23 QTLs located on 6D. Twenty-
209 three QTLs were identified under the low N treatment and 32 for the high N treatment. Nine
210 QTLs were found to be only present in the low N treatment, 18 QTLs were found only in the
211 high N treatment and 14 QTLs (28 total) were present in both N treatments. Phenotypic
212 variation explained by QTLs varied from 3.8 to 82.9%. Of the QTLs found, N treatment
213 dependent root angle QTLs (RAE1001/751, LOD 3.0/2.6 respectively) were identified on
214 chromosomes 2D, 3B and 4D. Nitrogen-dependent root size QTLs were found on
215 chromosomes 1A, 6D and 7D. For chromosomes 6D and 7D, N treatment independent QTLs
216 were found for root size and vigour. N-dependent QTLs were also found on chromosomes 6D
217 and 7D that co-localised with other N independent root size QTLs.

218 *RNA-seq analysis*

219 A seminal root QTL (RAE1001) was selected for RNA-sequencing analysis as it had the
220 smallest peak confidence region (25 cM) for an N-dependent QTL (Table 4). As there was no

221 single clear enriched region from the QTL analyses for the trait, the whole chromosome was
222 considered for analysis. A total of 3299 differentially expressed genes were identified in the
223 analysed groups. 1857 differentially expressed genes showed significant ($p < 0.05$) up-
224 regulation in Group A (with the QTL) compared to Group B (without QTL). Of these, 88
225 gene candidates resided on chromosome 2D. Additionally, MaSuRcA transcript assemblies
226 were considered that were identified as significantly ($p < 0.05$) up-regulated in Group A
227 compared Group B on chromosome 2D bringing the total to 93 (88 plus five) differentially
228 expressed candidate sequences (Table S2). The inclusion of these *de novo* assembled
229 transcript sequences in the analysis factors for varietal specific genes responsible for this
230 phenotype that are not present in the Chinese Spring based reference sequences. Of the 93
231 differentially expressed candidate sequences, 17 candidate genes were consistently expressed
232 across the Group A replicates verses zero reads mapping in one or more Group B replicates
233 and were therefore considered as our primary candidates (Table 4). There were also 1442
234 differentially expressed genes that showed significant ($p < 0.05$) down-regulation in Group A
235 (with the QTL) compared to Group B (without QTL). Of these, 65 were annotated as residing
236 on chromosome 2D (Table S2).

237 *Phylogenetic analysis*

238 For the candidate N-dependent root angle QTL (RAE1001) an upregulated NPF family gene,
239 TraesCS2D02G348400, was identified. A phylogenetic analysis of protein families was
240 conducted comparing NPF family protein sequences of *A. thaliana*, *O. sativa L.* and *T.*
241 *aestivum L.* (Fig. S2). A total of 53 *A. thaliana* proteins, 130 *O. sativa L.* proteins and 391 *T.*
242 *aestivum L.* proteins were aligned using MUSCLE with 1000 bootstrap interactions and 20
243 maximum likelihood searches (Edgar, 2004). The candidate *T. aestivum L.* protein
244 TraesCS2D02G348400 is situated in a monocot specific sub-clade within the NPF4 clade
245 (Fig. 3). This clade includes *A. thaliana* NPF members AtNPF4.1, AtNPF4.2, AtNPF4.3,
246 AtNPF4.4, AtNPF4.5, AtNPF4.6 and AtNPF4.7. In addition, the candidate protein is closely
247 related to a rice nitrate(chlorate)/proton symporter protein LOC_Os04g41410.

248 **Discussion**

249 *N-treatment dependent root QTLs*

250 In this study, a total of 55 QTLs were discovered for seedling root traits across both N
251 treatments (LOD > 2.0) (Fig. 2, Table 3). Of these loci, nine root QTLs were only detected in
252 the low N treatment, 18 QTLs were found only in the high N treatment and 14 QTLs (28
253 total) were present in both N treatments.

254

255 In the literature, there are previously described QTL regions associated with architectural root
256 traits. On chromosome 1A QTL were found in this study for lateral root traits under low N
257 conditions. Interestingly chromosome 1A has been previously associated with lateral root
258 length in wheat and rice (Ren *et al.*, 2012; Beyer *et al.*, 2018). It appears that there are
259 underlying genes on chromosome 1A that could be related to plasticity, tolerance and/or
260 lateral root development (An *et al.*, 2006; Landjeva *et al.*, 2008; Ren *et al.*, 2012; Guo *et al.*,
261 2012; Zhang *et al.*, 2013; Liu *et al.*, 2013; Sun *et al.*, 2013). This region has also been
262 correlated to NUp in S×R field trials (Atkinson *et al.*, 2015) which would make the
263 chromosome region an important candidate for further study. On chromosomes 2D, 3B and
264 4D, N-dependent root angle QTLs were identified in wheat grown in hydroponics. QTLs on
265 these chromosomes have been described in other studies but very few of these have measured
266 root angle or distribution traits. From comparison with other studies that found root QTLs on
267 chromosome 2D it appears there is an underlying gene for seminal root development and/or
268 plasticity (An *et al.*, 2006; Zhang *et al.*, 2013; Liu *et al.*, 2013). For chromosome 3B, other
269 studies have found QTLs affecting root size and stress related traits or genes relating to N
270 plasticity, uptake or mobilisation (An *et al.*, 2006; Habash *et al.*, 2007; Guo *et al.*, 2012;
271 Zhang *et al.*, 2013; Bai *et al.*, 2013). For chromosome 4D, comparing with other studies that
272 found QTLs on this chromosome there appears to be an underlying root development and/or
273 root plasticity gene (Zhang *et al.*, 2013; Bai *et al.*, 2013).

274

275 *RNA-sequencing of candidate root QTL*

276 A low N-treatment dependent seminal root angle QTL (LOD 3.0) on chromosome 2D was
277 targeted for transcriptomic analysis. A total of 17 candidate upregulated genes were identified
278 that were upregulated in this region (Table 4). A more detailed list of the genes identified are

279 given in Fig. S2. Two of the three genes with highest log changes plus four others have
280 unknown function. Point mutation detection and mutant generation with TILLING or RNAi
281 represent the next step to functionally characterise these genes.

282

283 One promising candidate from root transcriptomic analyses was a nitrate transporter
284 1/peptide transporter (NPF) family gene, NPF4 (TraesCS2D02G348400). This gene was
285 upregulated in a N-dependent manner related to a root angle QTL. In *A. thaliana* and *O.*
286 *sativa L.*, NPF family genes have important roles in lateral root initiation, branching and
287 response to nitrate (Remans *et al.*, 2006; Krouk *et al.*, 2010; Fang *et al.*, 2013). However, no
288 studies have reported genes controlling root angle change in wheat, to date. A phylogenetic
289 analysis of protein families was conducted comparing the protein sequences of *A. thaliana*,
290 *O. sativa L.* and *T. aestivum L.* to the candidate protein. The candidate *T. aestivum L.* protein
291 is situated in a monocot specific sub-clade within the NPF4 clade and is closely related to a
292 rice nitrate(chlorate)/proton symporter protein (LOC_Os04g41410) (Fig. 3). Members of this
293 clade are known for transporting the plant hormone abscisic acid (ABA) (AtNPF4.1 and
294 AtNPF4.6) and have been demonstrated to have low affinity nitrate transport activity
295 (AtNPF4.6) (Huang *et al.*, 1999; Kanno *et al.*, 2012). ABA is known to be a key regulator in
296 root hydrotropism, a process that senses and drives differential growth towards preferential
297 water potential gradients (Antoni *et al.*, 2016; Takahashi *et al.*, 2002). Hydrotropism has been
298 demonstrated to be independent of the auxin induced gravitropism pathway and can compete
299 in root angle changes against gravity (Dietrich *et al.*, 2018). Based on the experiments
300 presented here, we propose that the enhanced ABA flux via the upregulated NPF4 gene could
301 be driving a low N-dependent shallow root angle change while competing with the
302 gravitropism pathway. As root angle is a determinant of root depth, pursuing this gene
303 function is important agronomically for improving foraging capacity and uptake of nitrate in
304 deep soil layers.

305

306 In summary, we found 55 root QTLs using a wheat seedling hydroponic system, 25 of which
307 were N-treatment dependent. Using transcriptome analyses we found an upregulated NPF
308 family gene likely transporting nitrate or ABA as part of a N-dependent response affecting
309 root angle. These findings provide a valuable genetic insight for root angle control, N-
310 dependent responses and candidate genes for improvement of N capture in wheat.

311 **Supplementary data**

312 **Table S1.** Composition of ¼ Hoagland's nutrient solution.

313 **Table S2.** Full list of up- and downregulated genes ($p < 0.05$) for a seminal root angle QTL
314 located on chromosome 2D.

315 **Fig. S1.** High-throughput hydroponic phenotyping system for seedling root & shoot traits.

316 (A) Growth assembly. (B) Image acquisition. (C) Example image of a wheat root grown on

317 germination paper 10 DAG. (D) Root system extraction to RSML database using RootNav

318 software. (E) Measurement of root traits from RSML database. (F) Example image of a wheat

319 shoot 10 DAG. (G) Shoot image colour thresholding & shoot measurement using Fiji. (H)

320 Example of QTL peak extracted from phenotyping data & mapping data with rQTL.

321 **Fig. S2.** Phylogenetic tree of protein families comparing the NPF family protein sequences of

322 *A. thaliana*, *O. sativa* L. and *T. aestivum* L.

323 **Acknowledgements**

324 This work was supported by the Biotechnology and Biological Sciences Research Council
325 [grant number BB/M001806/1, BB/L026848/1, BB/P026834/1] (MJB, DMW, and MPP); the
326 Leverhulme Trust [grant number RPG-2016-409] (MJB and DMW); the European Research
327 Council FUTUREROOTS Advanced Investigator grant [grant number 294729] to MG, JAA,
328 DMW, and MJB; and the University of Nottingham Future Food Beacon of Excellence. The
329 authors would like to thank Limagrain UK Ltd for the use of the S×R DH population and
330 Luzie U. Wingen (John Innes Centre) for providing rQTL scripts used in this work.

References

- Akpinar BA, Kantar M, Budak H.** 2015. Root precursors of microRNAs in wild emmer and modern wheats show major differences in response to drought stress. *Functional & Integrative Genomics* **15**, 587–598.
- An D, Su J, Liu Q, Zhu Y, Tong Y, Li J, Jing R, Li B, Li Z.** 2006. Mapping QTLs for nitrogen uptake in relation to the early growth of wheat (*Triticum aestivum* L.). *Plant and Soil* **284**, 73–84.
- Anders S, Huber W.** 2010. Differential expression analysis for sequence count data. *Genome biology* **11**, R106.
- Atkinson JA, Wingen LU, Griffiths M, Pound MP, Gaju O, Foulkes MJ, Le Gouis J, Griffiths S, Bennett MJ, King J, et al.** 2015. Phenotyping pipeline reveals major seedling root growth QTL in hexaploid wheat. *Journal of Experimental Botany* **66**, 2283–2292.
- Bai C, Liang Y, Hawkesford MJ.** 2013. Identification of QTLs associated with seedling root traits and their correlation with plant height in wheat. *Journal of Experimental Botany* **64**, 1745–1753.
- Beyer S, Daba S, Tyagi P, Bockelman H, Brown-Guedira G, Mohammadi M.** 2018. Loci and candidate genes controlling root traits in wheat seedlings—a wheat root GWAS. *Functional & Integrative Genomics*.
- Bolger AM, Lohse M, Usadel B.** 2014. Trimmomatic: a flexible trimmer for Illumina sequence data. *Bioinformatics* **30**, 2114–2120.
- Broman KW, Wu H, Sen S, Churchill GA.** 2003. R/qtl: QTL mapping in experimental crosses. *Bioinformatics* **19**, 889–890.
- Churchill GA, Doerge RW.** 1994. Empirical Threshold Values for Quantitative Trait Mapping. *Genetics* **138**, 963–971.
- Clark RT, Famoso AN, Zhao K, Shaff JE, Craft EJ, Bustamante CD, Mccouch SR, Aneshansley DJ, Kochian LV.** 2013. High-throughput two-dimensional root system phenotyping platform facilitates genetic analysis of root growth and development: Root phenotyping platform. *Plant, Cell & Environment* **36**, 454–466.
- Dawson J C, Huggins DR, Jones SS.** 2008. Characterizing nitrogen use efficiency in natural and agricultural ecosystems to improve the performance of cereal crops in low-input and organic agricultural systems. *Field Crops Research* **107**, 89–101.
- Delogu G, Cattivelli L, Pecchioni N, De Falcis D, Maggiore T, Stanca AM.** 1998. Uptake and agronomic efficiency of nitrogen in winter barley and winter wheat. *European Journal of Agronomy* **9**, 11–20.
- Edgar R C.** 2004. MUSCLE: multiple sequence alignment with high accuracy and high throughput. *Nucleic Acids Research*. **32**, 1792–1797.

El-Gebali S, Mistry J, Bateman A, Eddy SR, Luciani A, Potter SC, Qureshi M, Richardson LJ, Salazar GA, Smart A, et al. 2019. The Pfam protein families database in 2019. *Nucleic Acids Research* **47**, D427–D432.

Fang Z, Xia K, Yang X, Grottemeyer MS, Meier S, Rentsch D, Xu X, Zhang M. 2013. Altered expression of the PTR/NRT1 homologue OsPTR9 affects nitrogen utilization efficiency, growth and grain yield in rice. *Plant Biotechnology Journal* **11**, 446–458.

FAO. 2017. World fertilizer Trends and Outlook to 2020. Food and Agriculture Organization of the United Nations. Rome, Italy. Available online at: <http://www.fao.org/3/a-i6895e.pdf> (Accessed January 20, 2019).

Gelli M, Duo Y, Konda AR, Zhang C, Holding D, Dweikat I. 2014. Identification of differentially expressed genes between sorghum genotypes with contrasting nitrogen stress tolerance by genome-wide transcriptional profiling. *BMC genomics* **15**, 179.

Guo Y, Kong F, Xu Y, Zhao Y, Liang X, Wang Y, An D, Li S. 2012. QTL mapping for seedling traits in wheat grown under varying concentrations of N, P and K nutrients. *Theoretical and Applied Genetics* **124**, 851–865.

Habash DZ, Bernard S, Schondelmaier J, Weyen J, Quarrie SA. 2007. The genetics of nitrogen use in hexaploid wheat: N utilisation, development and yield. *Theoretical and Applied Genetics* **114**, 403–419.

Haley CS, Knott SA. 1992. A simple regression method for mapping quantitative trait loci in line crosses using flanking markers. *Heredity* **69**, 315–324.

Hodge A, Berta G, Doussan C, Merchan F, Crespi M. 2009. Plant root growth, architecture and function. *Plant and Soil* **321**, 153–187.

Huang N-C, Liu K-H, Lo H-J, Tsay Y-F. 1999. Cloning and Functional Characterization of an Arabidopsis Nitrate Transporter Gene That Encodes a Constitutive Component of Low-Affinity Uptake. *The Plant Cell* **11**, 1381–1392.

International Wheat Genome Sequencing Consortium. 2018. Shifting the limits in wheat research and breeding using a fully annotated reference genome. *Science* **361**, eaar7191.

Kanno Y, Hanada A, Chiba Y, Ichikawa T, Nakazawa M, Matsui M, Koshiha T, Kamiya Y, Seo M. 2012. Identification of an abscisic acid transporter by functional screening using the receptor complex as a sensor. *Proceedings of the National Academy of Sciences* **109**, 9653–9658.

Kant S, Bi Y-M, Rothstein SJ. 2010. Understanding plant response to nitrogen limitation for the improvement of crop nitrogen use efficiency. *Journal of Experimental Botany* **62**, 1499–1509.

Kawahara Y, de la Bastide M, Hamilton JP, Kanamori H, McCombie WR, Ouyang S, Schwartz DC, Tanaka T, Wu J, Zhou S, et al. 2013. Improvement of the *Oryza sativa* Nipponbare reference genome using next generation sequence and optical map data. *Rice* **6**, 4.

- Krogh A, Larsson B, von Heijne G, Sonnhammer EL.** 2001. Predicting transmembrane protein topology with a hidden markov model: application to complete genomes. *Journal of Molecular Biology* **305**, 567–580.
- Krouk G, Crawford NM, Coruzzi GM, Tsay Y-F.** 2010. Nitrate signaling: adaptation to fluctuating environments. *Current Opinion in Plant Biology* **13**, 265–272.
- Landjeva S, Neumann K, Lohwasser U, Börner A.** 2008. Molecular mapping of genomic regions associated with wheat seedling growth under osmotic stress. *Biologia Plantarum* **52**, 259–266.
- Léran S, Varala K, Boyer J-C, Chiurazzi M, Crawford N, Daniel-Vedele F, David L, Dickstein R, Fernandez E, Forde B, et al.** 2014. A unified nomenclature of NITRATE TRANSPORTER 1/PEPTIDE TRANSPORTER family members in plants. *Trends in Plant Science* **19**, 5–9.
- Liu X, Li R, Chang X, Jing R.** 2013. Mapping QTLs for seedling root traits in a doubled haploid wheat population under different water regimes. *Euphytica* **189**, 51–66.
- Lobet G, Pound MP, Diener J, Pradal C, Draye X, Godin C, Javaux M, Leitner D, Meunier F, Nacry P, et al.** 2015. Root System Markup Language: Toward a Unified Root Architecture Description Language. *Plant Physiology* **167**, 617–627.
- Oono Y, Kawahara Y, Yazawa T, Kanamori H, Kuramata M, Yamagata H, Hosokawa S, Minami H, Ishikawa S, Wu J, et al.** 2013. Diversity in the complexity of phosphate starvation transcriptomes among rice cultivars based on RNA-Seq profiles. *Plant Molecular Biology* **83**, 523–537.
- Ouellette LA, Reid RW, Blanchard SG, Brouwer CR.** 2018. LinkageMapView—rendering high-resolution linkage and QTL maps (O Stegle, Ed.). *Bioinformatics* **34**, 306–307.
- Pertea M, Kim D, Pertea GM, Leek JT, Salzberg SL.** 2016. Transcript-level expression analysis of RNA-seq experiments with HISAT, StringTie and Ballgown. *Nature Protocols* **11**, 1650–1667.
- Pound MP, French AP, Atkinson JA, Wells DM, Bennett MJ, Pridmore T.** 2013. RootNav: Navigating Images of Complex Root Architectures. *Plant Physiology* **162**, 1802–1814.
- Remans T, Nacry P, Pervent M, Filleur S, Diatloff E, Mounier E, Tillard P, Forde BG, Gojon A.** 2006. The Arabidopsis NRT1. 1 transporter participates in the signaling pathway triggering root colonization of nitrate-rich patches. *Proceedings of the National Academy of Sciences* **103**, 19206–19211.
- Ren Y, He X, Liu D, Li J, Zhao X, Li B, Tong Y, Zhang A, Li Z.** 2012. Major quantitative trait loci for seminal root morphology of wheat seedlings. *Molecular Breeding* **30**, 139–148.
- Schindelin J, Arganda-Carreras I, Frise E, Kaynig V, Longair M, Pietzsch T, Preibisch S, Rueden C, Saalfeld S, Schmid B, et al.** 2012. Fiji: an open-source platform for biological-image analysis. *Nature Methods* **9**, 676–682.

Stamatakis A. 2014. RAxML version 8: a tool for phylogenetic analysis and post-analysis of large phylogenies. *Bioinformatics* **30**, 1312–1313.

Sun J, Guo Y, Zhang G, Gao M, Zhang G, Kong F, Zhao Y, Li S. 2013. QTL mapping for seedling traits under different nitrogen forms in wheat. *Euphytica* **191**, 317–331.

Wang J, Luo M-C, Chen Z, You FM, Wei Y, Zheng Y, Dvorak J. 2013. *Aegilops tauschii* single nucleotide polymorphisms shed light on the origins of wheat D-genome genetic diversity and pinpoint the geographic origin of hexaploid wheat. *New Phytologist* **198**, 925–937.

Yu P, Eggert K, von Wirén N, Li C, Hochholdinger F. 2015. Cell Type-Specific Gene Expression Analyses by RNA Sequencing Reveal Local High Nitrate-Triggered Lateral Root Initiation in Shoot-Borne Roots of Maize by Modulating Auxin-Related Cell Cycle Regulation. *Plant Physiology* **169**, 690–704.

Yu G, Smith DK, Zhu H, Guan Y, Lam TT-Y. 2017. ggtree: an r package for visualization and annotation of phylogenetic trees with their covariates and other associated data (G McInerny, Ed.). *Methods in Ecology and Evolution* **8**, 28–36.

Zhang H, Cui FA, Wang LIN, Li JUN, Ding A, Zhao C, Bao Y, Yang Q, Wang H. 2013. Conditional and unconditional QTL mapping of drought-tolerance-related traits of wheat seedling using two related RIL populations. *Journal of genetics* **92**, 213–231.

Zimin AV, Marçais G, Puiu D, Roberts M, Salzberg SL, Yorke JA. 2013. The MaSuRCA genome assembler. *Bioinformatics* **29**, 2669–2677.

Zurek PR, Topp CN, Benfey PN. 2015. Quantitative Trait Locus Mapping Reveals Regions of the Maize Genome Controlling Root System Architecture. *Plant Physiology* **167**, 1487–1496.

Table 1. Definition of root traits measured using RootNav.

Acronym	Definition	Software	Units
RTLA	Total length of all roots	RootNav	mm
RTLS	Total length of seminal roots	RootNav	mm
RTLL	Total length of lateral roots	RootNav	mm
RSC	Number of seminal roots	RootNav	Dimensionless (Count)
RLC	Number of lateral roots	RootNav	Dimensionless (Count)
RMW	Maximum width of the root system	RootNav	mm
RMD	Maximum depth of the root system	RootNav	mm
RWDR	Width-depth ratio (MW/MD)	RootNav	Dimensionless (Ratio)
RCMX	Root centre of mass- horizontal co-ordinate	RootNav	mm
RCMY	Root centre of mass - vertical co-ordinate	RootNav	mm
RCH	Convex hull - area of the smallest convex polygon to enclose the root system	RootNav	mm ²
RCHCX	Convex hull centroid - horizontal co-ordinate	RootNav	mm
RCHCY	Convex hull centroid - vertical co-ordinate	RootNav	mm
RAE1	Angle of emergence between the outermost seminal roots measured at 30 px	RootNav	Degrees (°)
RAE2	Angle of emergence between innermost pair of seminal roots measured at 30 px	RootNav	Degrees (°)
RAE951	Angle of emergence between outermost pair of seminal roots measured at 95 px	RootNav	Degrees (°)
RAE952	Angle of emergence between innermost pair of seminal roots measured at 95 px	RootNav	Degrees (°)
RAE251	Angle of emergence between outermost pair of seminal roots measured at first quartile of total length	RootNav	Degrees (°)
RAE252	Angle of emergence between innermost pair of seminal roots measured at first quartile of total length	RootNav	Degrees (°)
RAE501	Angle of emergence between outermost pair of seminal roots measured at second quartile of total length	RootNav	Degrees (°)
RAE502	Angle of emergence between innermost pair of seminal roots measured at first quartile of total length	RootNav	Degrees (°)
RAE751	Angle of emergence between outermost pair of seminal roots measured at third quartile of total length	RootNav	Degrees (°)
RAE752	Angle of emergence between innermost pair of seminal roots measured at third quartile of total length	RootNav	Degrees (°)
RAE1001	Angle of emergence between outermost pair of seminal roots measured at root tip	RootNav	Degrees (°)
RAE1002	Angle of emergence between innermost pair of seminal roots measured at root tip	RootNav	Degrees (°)
SH	Shoot height	FIJI	mm
SA	Shoot area	FIJI	mm ²

Table 2. Seedling phenotypic values for the S×R doubled haploid population and parents under two N regimes ($n = 18$, range = 8 to 36). Trait units as Table 1. Note: shoot data available for low N treatment only.

Trait	Treat	Savannah	Rialto	DH population			
		Mean ± SE	Mean ± SE	Mean ± SE	Range	Kurt	Skew
TLA	LN	536 ± 49	360.4 ± 24	485.7 ± 28	286.1 – 891	-0.5	0.5
	HN	668 ± 48	360 ± 28	479 ± 27	244 – 811	-0.5	0.3
TLS	LN	503 ± 39	353 ± 24	461 ± 24	280 – 791	-0.8	0.4
	HN	574 ± 32	345 ± 25	448 ± 23	240 – 651	-1	0
TLL	LN	33 ± 14	7.5 ± 2	25 ± 5	2.6 – 99	1.6	1.5
	HN	94.6 ± 23	15.4 ± 5	31.4 ± 6	1.5 – 176	7.1	2.3
RAE1	LN	85.7 ± 9	93.3 ± 6	92.4 ± 2	70 – 121	0.3	0.5
	HN	101 ± 10	103 ± 7	93.1 ± 4	56.7 – 140	0.3	0.4
RAE2	LN	49.1 ± 12	55.4 ± 6	60.5 ± 2	38.9 – 85	1.2	0.3
	HN	73.5 ± 6	62.8 ± 8	62.9 ± 2	39.7 – 95	0.3	0.5
LRC	LN	11.6 ± 7	4 ± 2	9.7 ± 1	1.7 – 28	0.6	1.2
	HN	20.9 ± 4	4.9 ± 1	9.1 ± 1	0.5 – 39	3.7	1.7
SRC	LN	4.7 ± 0.3	4.8 ± 0.1	4.6 ± 0.1	3.8 – 5	-0.1	-0.4
	HN	4.7 ± 0.2	5.2 ± 0.1	4.7 ± 0.1	3.8 – 5	0	-0.6
RCH	LN	11216 ± 2759	4540 ± 700	8893 ± 1015	2824 – 21774	-0.4	0.7
	HN	17832 ± 2498	4193 ± 792	9026 ± 950	2530 – 22836	-0.1	0.7
RMW	LN	108 ± 21	68.9 ± 7	94.3 ± 6	52.4 – 161	-0.7	0.5
	HN	138 ± 15	71.8 ± 7	89 ± 5	55.1 – 158	-0.2	0.7
RMD	LN	177 ± 15	113 ± 8	154 ± 8	94.7 – 240	-1.3	0.3
	HN	232 ± 15	118 ± 9	165 ± 8	89.5 – 246	-0.8	0
RWD	LN	0.6 ± 0.1	0.6 ± 0.1	0.6 ± 0	0.4 – 1	0.1	-0.2
	HN	0.6 ± 0.1	0.6 ± 0.1	0.6 ± 0	0.3 – 1	0.6	0.2
RCMX	LN	-0.9 ± 3	-3.4 ± 2	-2.7 ± 1	-14.2 – 2	3.3	-1.1
	HN	-2.3 ± 2	-0.5 ± 2	-1.9 ± 0	-9.6 – 1	0.9	-0.9
RCMY	LN	55.1 ± 4	36 ± 3	49.6 ± 3	29.2 – 73	-1.4	0.1
	HN	61.2 ± 3	30.6 ± 3	50.3 ± 3	23.5 – 73	-1	-0.2
RCHCX	LN	1.4 ± 5	-4.4 ± 2	-4.4 ± 1	-19.2 – 3	1.9	-0.9
	HN	-4.2 ± 5	-0.5 ± 2	-4.1 ± 1	-13.5 – 2	-0.6	-0.4
RCHCY	LN	85.3 ± 9	52.1 ± 4	74.2 ± 5	41.9 – 119	-1.3	0.3
	HN	103 ± 6	46.9 ± 4	76.2 ± 4	34.8 – 121	-0.9	0
RAE951	LN	81.4 ± 11	83.8 ± 6	82.2 ± 2	63.4 – 104	-0.1	0.1
	HN	95.9 ± 8	93.9 ± 6	87.9 ± 2	59.6 – 112	0	-0.3
RAE952	LN	46.7 ± 12	48.4 ± 5	51.9 ± 2	34.2 – 72	0	0
	HN	68.5 ± 9	54.4 ± 7	58.9 ± 2	35 – 88	0.4	0.2
RAE251	LN	76.8 ± 12	85.4 ± 6	78.5 ± 2	59.7 – 94	-0.5	-0.2
	HN	89.4 ± 7	92.2 ± 6	84 ± 2	60.2 – 104	-0.1	-0.2
RAE252	LN	50.4 ± 12	48.6 ± 5	49.1 ± 1	29.5 – 63	-0.4	-0.2
	HN	63.1 ± 8	55.9 ± 6	56.1 ± 2	36.8 – 83	0.1	0.3

RAE501	LN	71.8 ± 13	78.9 ± 6	73.2 ± 2	53.8 – 90	-0.2	0
	HN	87.9 ± 7	85.4 ± 7	79.4 ± 2	59.3 – 99	-0.1	-0.2
RAE502	LN	49.1 ± 10	47.5 ± 4	46.2 ± 1	28.7 – 61	-0.2	0
	HN	56.4 ± 9	54.8 ± 5	50.4 ± 2	28.2 – 70	-0.1	0
RAE751	LN	69.1 ± 12	74.7 ± 6	71.8 ± 2	56.6 – 91	0.2	0.3
	HN	87.2 ± 8	81.6 ± 7	76.7 ± 2	55.6 – 96	0	-0.1
RAE752	LN	50 ± 9	46 ± 4	46 ± 1	30.4 – 59	-0.2	0
	HN	53.7 ± 9	49.4 ± 6	47 ± 2	26.6 – 63	-0.3	-0.2
RAE1001	LN	68.6 ± 11	71.6 ± 6	71.3 ± 2	55.7 – 92	0.5	0.5
	HN	87.2 ± 8	76.5 ± 7	74.4 ± 2	53.2 – 97	0.4	0
RAE1002	LN	49.3 ± 8	43.8 ± 4	45.4 ± 1	32 – 59	-0.2	-0.1
	HN	51.8 ± 8	42.5 ± 6	43.5 ± 2	21.4 – 59	0.2	-0.4
SH	LN	72.4 ± 7	69.1 ± 3	75.8 ± 0	51 – 90	0.2	-0.4
SA	LN	137.9 ± 8	153.7 ± 5	165.8 ± 1	85.4 – 271	0.2	-0.4

Table 3. QTLs for wheat seedling traits detected in the S×R DH population grown in hydroponics. Trait units as Table 1. Note: shoot data available for low N treatment only.

Trait	Treat	QTL	Interval ^a	Site ^b		H ² ^e	
				(cM)	LOD ^c	Additive ^d	(%)
RTLA	LN	6D	BobWhite_c7090_522-BS00023964	5.0	27.4	-229	65.0
		7D	wsnp_Ku_c416_869895-BS00028760_51	26.0	8.4	-107	11.3
	HN	6D	BobWhite_c7090_522-BS00023964	4.4	23.0	-1275	57.4
		7D	wsnp_Ku_c416_869895-BS00028760_51	27.0	8.7	-703	14.3
RTLS	LN	6D	BobWhite_c7090_522-BS00023964	5.0	33.5	-198	70.5
		7D	wsnp_Ku_c416_869895-BS00028760_51	26.0	11.3	-86	12.1
	HN	6D	BobWhite_c7090_522-BS00023964	4.4	24.8	-1068	59.9
		7D	wsnp_Ku_c416_869895-BS00028760_51	27.0	9.4	-580	14.4
RTLL	LN	1A	BS00004043-BS00000226	215.0	2.3	-9.0	6.2
		6D	BobWhite_c7090_522-BS00023964	8.0	13.4	-31.2	48.0
	HN	6D	BS00009514-BS00023964 BobWhite_c22370_352-	4.4	6.3	-208	28.0
RAE1	HN	3B	wsnp_RFL_Contig3336_3426054 GENE-1154_396-	178.8	2.2	-11.0	10.8
RAE2	HN	3B	wsnp_RFL_Contig3336_3426054	178.8	2.8	-8.2	13.3
RLC	LN	1A	BS00004043-BS00000226	216.0	4.9	-2.4	8.6
		6D	BobWhite_c7090_522-BS00023964	5.0	19.6	-9.4	52.8
		7D	wsnp_Ku_c416_869895-BS00028760_51	22.0	6.0	-4.4	10.9
RSC	LN	6D	BS00009514-BS00023964	4.4	8.8	-8.5	36.5
		7D	wsnp_Ku_c416_869895-IAAV4624 Excalibur_c48636_283-	23.0	3.8	-0.2	15.8
	HN	7A	wsnp_RFL_Contig2864_2688208	12.0	2.9	0.2	13.7
RCH	LN	6D	BobWhite_c7090_522-BS00023964	4.4	31.1	-8464	80.0
		6D	BobWhite_c7090_522-BS00023964	4.4	18.4	-287837	53.5
	7D	wsnp_Ku_c416_869895-Kukri_c46303_512	34.0	4.2	-133799	8.3	
RMW	LN	1B	IAAV3905-wsnp_RFL_Contig3951_4390396	12.5	3.6	-8.9	5.0
		6D	BobWhite_c7090_522-BS00023964 wsnp_Ex_c9440_15657149-	4.4	26.7	-48.5	72.8
	HN	4D	wsnp_Ku_c16354_25219645	23.9	3.1	68.8	7.1
RMD	LN	6D	BS00009514-BS00023964	4.4	16.4	-230	54.6
		6D	BobWhite_c7090_522-BS00023964	4.4	31.5	-71.4	75.1
	7D	wsnp_Ku_c416_869895-BS00021859	27.0	3.7	-20.6	3.8	
		6D	BobWhite_c7090_522-BS00023964	4.4	21.8	-384	58.8
7D	wsnp_Ku_c416_869895-BS00028760_51	30.0	5.2	-169	8.6		
RMWD	HN	4D	wsnp_Ex_c9440_15657149-BS00065168	4.8	3.1	0.1	14.6
RCMX	LN	6D	BS00009514-BS00023964	6.0	2.3	1.6	11.2

	HN	1A	GENE-0249_122-BS00075532_51	145.0	4.1	-11.1	16.6
		6D	BS00009514-BS00023964	22.0	4.0	9.8	16.3
RCMY	LN	6D	BobWhite_c7090_522-BS00023964	4.4	31.9	-23.1	80.8
	HN	6D	BobWhite_c7090_522-BS00023964	4.4	19.5	-123	63.5
RCHCX	LN	6D	BS00009514-BS00023964	4.4	2.3	2.5	11.2
	HN	6D	BS00009514-BS00023964	18.0	3.2	13.6	12.9
		7D	wsnp_Ku_c416_869895-IAAV4624	21.0	3.2	16.5	13.1
RCHCY	LN	6D	BobWhite_c7090_522-BS00023964	4.4	34.1	-40.0	82.9
	HN	3B	BS00064778-BS00075879	216.2	4.9	45.2	6.8
		6D	BobWhite_c7090_522-BS00023964	4.4	25.0	-215.8	62.1
		7D	wsnp_Ku_c416_869895-Kukri_c46303_512	32.0	5.8	-91.8	8.2
			RAC875_c5799_224-				
RAE951	HN	3B	wsnp_Ra_c7158_12394405	178.8	2.8	-7.7	13.3
RAE251	LN	2D	BS00049876_51-BS00066132_51	117.0	1.4	3.8	7.1
			BobWhite_c22370_352-				
	HN	3B	wsnp_CAP11_c323_263800	178.8	3.6	-7.7	17.0
RAE252	HN	4D	wsnp_Ex_c9440_15657149-BS00065168	0.8	2.8	6.5	13.4
RAE501	HN	4D	wsnp_Ex_c9440_15657149-BS00065168	0.8	2.9	6.3	14.0
RAE502	HN	4D	wsnp_Ex_c9440_15657149-BS00065168	0.8	3.0	6.4	14.2
RAE751	LN	2D	BS00010393-BS00066132_51	160.0	2.6	5.1	12.5
	HN	4D	wsnp_Ex_c9440_15657149-BS00024014	0.8	2.9	6.3	13.8
RAE752	HN	4D	wsnp_Ex_c9440_15657149-BS00065168	0.8	2.1	5.3	10.4
RAE1001	LN	2D	BS00010393-BS00066132_51	160.0	3.0	5.5	14.3
	HN	4D	wsnp_Ex_c9440_15657149-BS00024014	0.8	2.4	6.0	11.9

^a Chromosome region of the QTL defined by two flanking markers

^b Genetic position of the QTL peak value

^c Logarithm of the odds value

^d Additive effects of putative QTL; a positive value indicates that positive alleles are from Savannah; negative values indicate positive alleles are from Rialto

^e Trait heritability

Table 4. Candidate genes for seminal root angle QTL located on chromosome 2D that were consistently expressed across the Group A replicates verses zero reads mapping in one or more Group B replicates. Gene naming convention according to IWGSC RefSeq v1.1.

Gene	Log ₂ fold change	p value	Functional annotation
TraesCS2D02G509700	1.73	0.002	Peroxidase
TraesCS2D02G344400	1.45	0.013	Unknown
MSTRG.42598 (TGACv1)	1.31	0.041	Unknown
TraesCS2D02G441300	1.29	0.037	AAA domain UvrD/REP helicase N-terminal domain
TraesCS2A02G111200	2.12	2.5E-05	Kelch motif
TraesCS2B02G126600	2.21	9.5E-06	Unknown
TraesCS2D02G487000	1.53	0.008	DUF wound-responsive family protein
TraesCS2D02G088100	1.29	0.036	C2H2-type zinc finger
TraesCS2D02G129100	1.36	0.036	Legume lectin domain
TraesCS2D02G330200	1.44	0.013	Unknown
MSTRG.40366 (TGACv1)	2.02	8.9E-05	Unknown
TraesCS2D02G108500	1.38	0.026	Peroxidase
TraesCS6A02G175000	1.66	0.002	Nuclear pore complex scaffold, nucleoporin
TraesCS2D02G270000	1.66	0.002	Helix-loop-helix DNA-binding domain
TraesCS2D02G511200	1.41	0.025	Peroxidase
TraesCS4B02G057100	1.48	0.013	Unknown
TraesCS2D02G348400	1.88	3.6E-04	NPF4

Figure legends

Fig. 1. Phenotypic variation in seedling traits for S×R doubled haploid under low high N treatments. Organised smallest (left) to largest (right) for low N treatment. (A) Total length of all roots (RTLA). (B) Total length of lateral roots (RTL). (C) Angle of emergence between outermost pair of seminal roots measured at root tip (RAE1001). ($n = 18$, range = 8 to 36).

Fig. 2. Molecular linkage map showing position of QTLs detected in the S×R DH population grown in hydroponics. QTLs and confidence regions for all root traits are colour labelled for low N-dependent (blue), high N-dependent (red) and N treatment independent (green) (LOD > 2.0).

Fig. 3. Phylogenetic tree of protein families comparing the protein sequences of *A. thaliana*, *O. sativa L.* and *T. aestivum L.* NPF family proteins to an identified candidate *T. aestivum L.* protein. The candidate *T. aestivum L.* protein is situated in a monocot specific outgroup within a NPF4 protein clade (highlighted in red). Branch lengths are proportional to substitution rate.

Fig. 1.

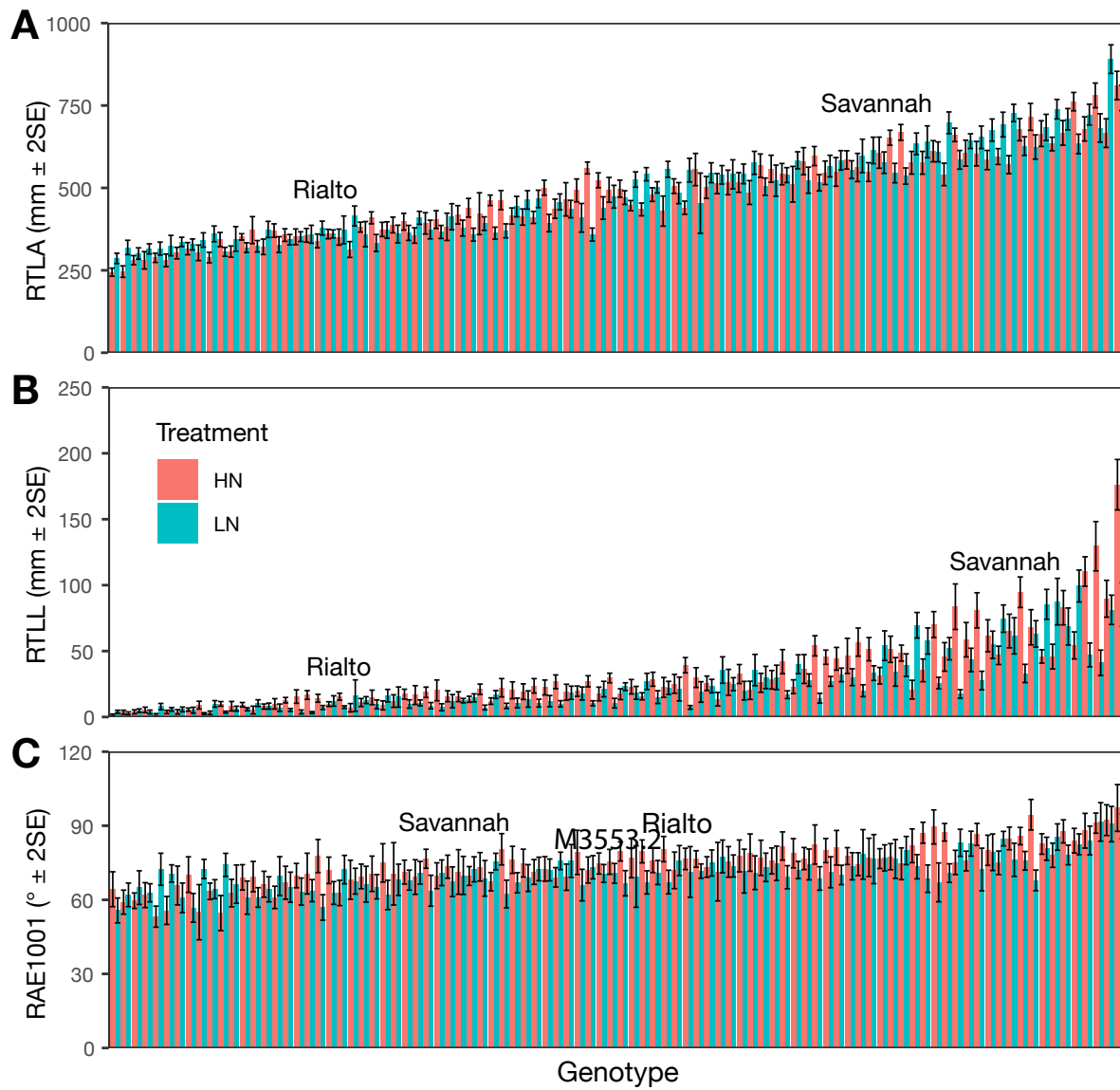


Fig. 2.

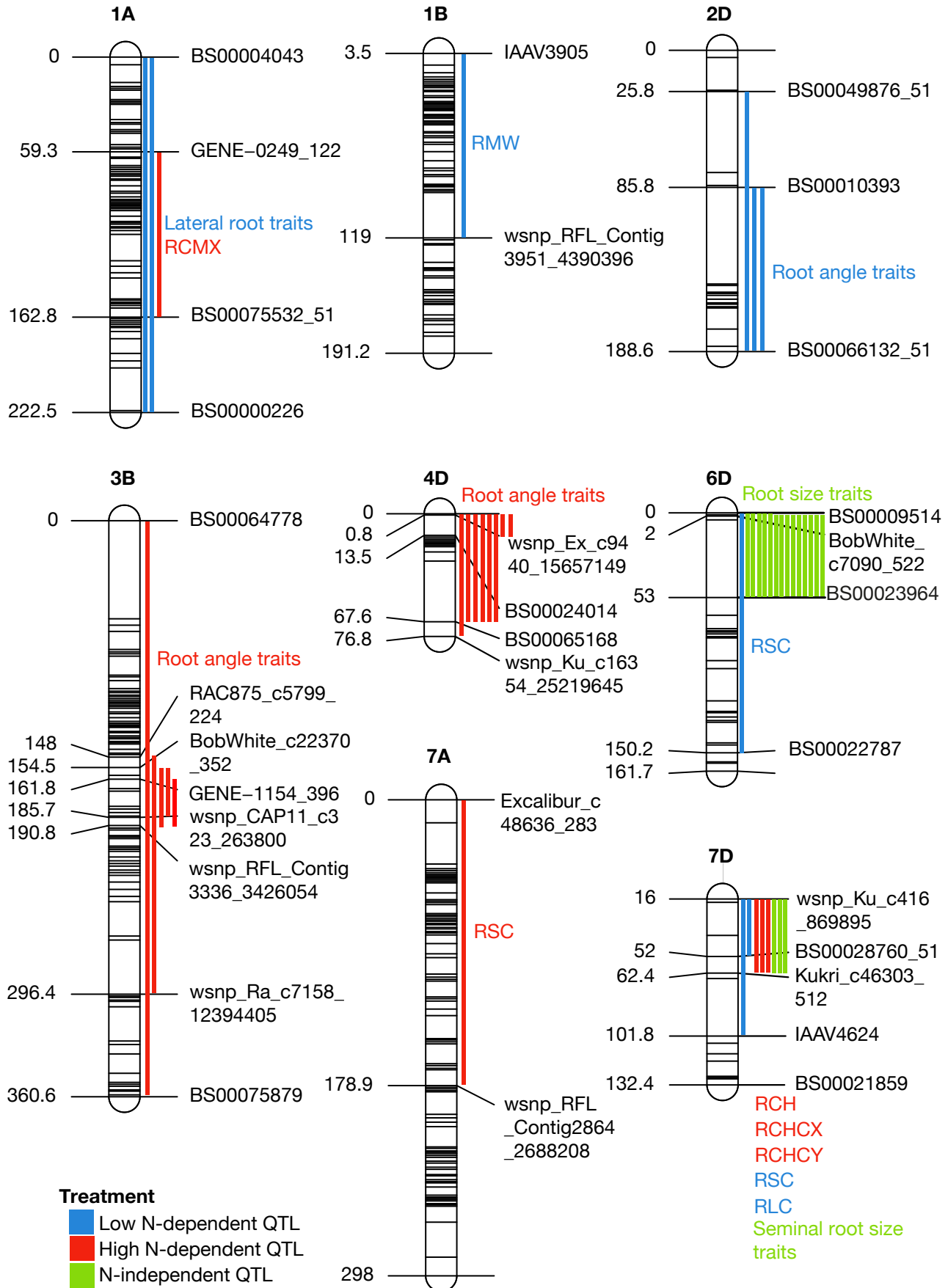


Fig. 3.

